Int. J. Multiphase Flow, Vol. 3, pp. 533–549. Pergamon/Elsevier, 1977. Printed in Great Britain

HEAT TRANSFER IN VERTICAL ANNULAR LAMINAR FLOW OF TWO IMMISCIBLE LIQUIDS

T. M. LEIB,† M. FINK‡ and D. HASSON
Department of Chemical Engineering, Technion–Israel Institute of Technology, Haifa, Israel

(*Received* 23 *December* 1976; *received for publication* 1 *July* 1977)

Abstract—The paper investigates heat transfer in annular laminar undisturbed flow of two immiscible liquids, with constant heat-flux generated at the wall of the tube. It presents an analytical solution for the fully developed temperature field. This is used to obtain a more general solution from a model, describing the temperature field as a superposition of the fully developed and the developing fields. This superposition model is solved by an orthogonal collocation method. An asymptotic model for short entry lengths is also described.

Calculations for a kerosene–water system, show that the superposition solution converges to the entrance solution below 100 diameters and converges asymptotically to the solution of the fully developed temperature field beyond 5000 diameters.

The effect of the wavy interface is assessed experimentally for annular kerosene–water flow, by comparing predicted and measured temperature profiles. It is found that experimental profiles are considerably flatter and measured Nusselt numbers for the kerosene phase are accordingly higher by 40–320% as compared to the undisturbed flow analyses.

1. INTRODUCTION

The laminar annular flow regime is rarely encountered in gas–liquid systems, but in liquid–liquid systems it can prevail over a significant range of flow rates (Hasson *et al.* 1974).

Problems of corrosion and fouling may conceivably be alleviated by having an immiscible liquid film such as kerosene flowing around a corrosive or fouling core of an aqueous liquid solution. In such a system heat-transfer to the core liquid could be deleteriously affected by the poor thermal conductivity of the wall liquid. The present study aims to explore the magnitude of this effect, while at the same time contributing to the fundamental understanding of heat transfer in laminar annular liquid–liquid flow.

The system of interest here is annular vertical flow of two liquids with unequal densities. Most studies deal with equal density liquids. It has been shown (Hasson *et al.* 1974) that small density differences may affect considerably the velocity field and hold-up in vertical liquid–liquid flow.

Previous heat-transfer studies provide solutions of the temperature field for annular laminar flow of equal density immiscible liquids, with constant wall temperature (Bentwich & Sideman 1964; Sideman & Peck 1965). The present study provides solutions for heat transfer in annular laminar flow of two immiscible liquids, with constant heat flux at the wall, taking into account density differences.

In this work, three heat transfer undisturbed flow models were studied: an asymptotic model for fully developed temperature field; an entrance model, applicable for short entry lengths, and a superposition model, applicable for the whole heated section.

An estimate of the effect of the wavy interface was obtained by referring to experimental measurements of temperature profiles.

2. METHODS OF SOLUTION

2.1. *General equations*

A control volume is considered (figure 1), bounded by the cylindrical surface of the tube's wall and by two cross sections of the pipe. The outer liquid is denoted by superscript (2) and

†At present with the Department of Chemical Engineering, University of Houston, Houston, Texas.
‡At present with the Atomic Energy Commission, Israel.

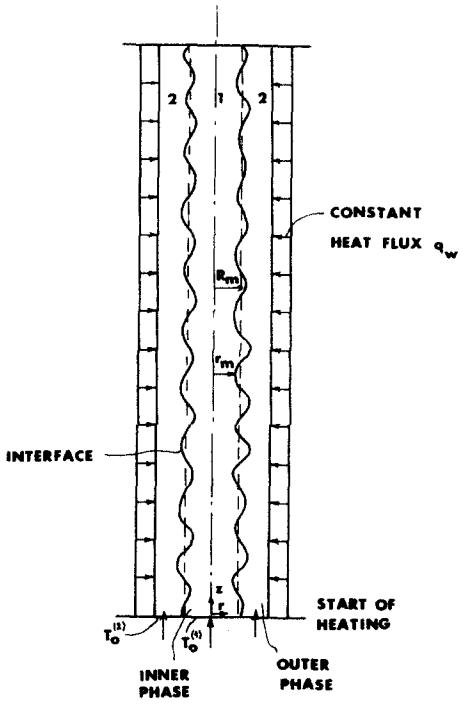

Figure 1. Heat transfer model in annular flow.

the inner liquid by superscript (1). The physical properties of each of the two fluids are taken at the average of the temperature range considered. A constant heat flux q_w is penetrating the wall of the tube at $r = R$, while the temperature of the inlet, at $z = 0$, is an arbitrary function of r, $T_0(r)$. It is assumed that the flow is fully developed throughout the heated section and that axial diffusion is negligible compared with axial convection. The interface is assumed to be undisturbed and cylindrical, being at a radial distance $r = R_m$ which is the average value calculated from the solution of the undisturbed flow field (Hasson *et al.* 1974).

The energy balance over the control volume yields:

$$v^{(i)}\frac{\partial T^{(i)}}{\partial z} = \alpha_t^{(i)}\frac{1}{r}\frac{\partial}{\partial r}\left[r\frac{\partial T^{(i)}}{\partial r}\right] \qquad 0 \le r \le R,\ z > 0. \qquad [1]$$

$\alpha_t^{(i)}$ are the thermal diffusivities of the liquids and $v^{(i)}$ are the velocity distributions, obtained by integration of the momentum balance equation (Hasson *et al.* 1974):

$$v^{(1)*} = \left\{M^{(1)}[\alpha^{(1)} - r^{*2}] + \frac{\mu^{(1)}}{\mu^{(2)}}v_m^{(2)*}\right\}, \qquad [2]$$

$$v^{(2)*} = [M^{(2)}(1 - r^{*2}) + \alpha^{(1)}\ln r^{*2}] \qquad [3]$$

where $\mu^{(i)}$ are liquid viscosities, $v^{(i)*}$ are dimensionless velocities, $M^{(i)}$ are dimensionless pressure drops, $N^{(i)}$ are dimensionless density differences, $\alpha^{(i)}$ are hold-up fractions, r^* is a dimensionless radial coordinate and $v_m^{(2)*}$ is the dimensionless interfacial velocity:

$$v^{(i)*} = \frac{v^{(i)}}{N^{(i)}}, \qquad [4]$$

$$r^* = \frac{r}{R}, \qquad [5]$$

$$\alpha^{(1)} = \left(\frac{R_m}{R}\right)^2, \tag{6}$$

$$\alpha^{(2)} = 1 - \alpha^{(1)}, \tag{7}$$

$$M^{(i)} = \frac{-\left[\frac{dP}{dz} + \rho^{(i)} g\right]}{N}, \tag{8}$$

$$N^{(i)} = \frac{NR^2}{4\mu^{(i)}}, \tag{9}$$

where P is the pressure, g is the gravitational acceleration and N is a dimensional density difference.

$$N = [\rho^{(1)} - \rho^{(2)}]g. \tag{10}$$

The boundary conditions are:

at $r = 0$

$$\frac{\partial T^{(1)}}{\partial r} = 0, \tag{11}$$

at $r = R_m$

$$T^{(1)} = T^{(2)}, \tag{12}$$

$$k^{(1)} \frac{\partial T^{(1)}}{\partial r} = k^{(2)} \frac{\partial T^{(2)}}{\partial r}, \tag{13}$$

at $r = R$

$$k^{(2)} \frac{\partial T^{(2)}}{\partial r} = -q_w. \tag{14}$$

The initial conditions are:

at $z = 0$

$$T^{(1)} = T_0^{(1)}, \tag{15}$$

$$T^{(2)} = T_0^{(2)}, \tag{16}$$

$k^{(i)}$ are the thermal conductivities and $T_0^{(i)}$ are the inlet temperature distributions.

2.2. *Asymptotic solution for the fully developed temperature field*

The fully developed temperature field will be denoted by subscript F (i.e. T_F). The differential equations [1] and the boundary conditions [11]–[14] remain unchanged, but [15]–[16] for initial conditions are replaced by the following overall energy balance:

$$\int_A \rho C_p v T_F \, dA - \int_{A_0} \rho C_p v T_0 \, dA = -2R\pi q_w z \tag{17}$$

where ρ is the density, C_p—the specific heat and A, A_0—the cross sectional areas at a distance z and at the inlet respectively.

The system of differential equations [1] with boundary conditions [11]–[14] and initial condition [17] is solved by separation of variables. The detailed solution is given by Fink (1975). The final equations, for uniform inlet temperatures, give the dimensionless temperature distributions as functions of the dimensionless radius $r^* = r/R$ and the dimensionless axial distance $z^* = z/D$ as follows:

$$T_F^{(1)*} = \left\{\left[M^{(1)}\alpha^{(1)} + \frac{\mu^{(1)}}{\mu^{(2)}} v_m^{(2)*}\right] r^{*2} - \frac{1}{4} M^{(1)} r^{*4}\right\} + C^{(1)} \cdot z^* + K \cdot P^{(1)}, \tag{18}$$

$$T_F^{(2)} = \left[M^{(2)}\left(r^{*2} - \frac{1}{4} r^{*4}\right) + \alpha^{(1)} r^{*2}(\ln r^{*2} - 2) + B \ln r^{*2}\right] + C^{(2)} \cdot z^* + L \cdot P^{(2)} \tag{19}$$

where the dimensionless temperatures $T_F^{(i)*}$ and the dimensionless constants $C^{(i)}$ are as follows:

$$T_F^{(i)*} = T_F^{(i)} \cdot P^{(i)}, \tag{20}$$

$$C^{(i)*} = \frac{32\mu^{(i)}\alpha_t^{(i)}}{NR^3}. \tag{21}$$

The dimensional constants $P^{(i)}$, a, B, K and L are as follows:

$$P^{(i)} = \frac{16\mu^{(i)}\alpha_t^{(i)}}{aNR^4}, \tag{22}$$

$$a = \frac{\dfrac{8q_w}{NR^3}\dfrac{\mu^{(2)}}{\rho^{(2)}C_p^{(2)}}}{\alpha^{(1)} - \dfrac{1}{2}M^{(2)} - B}, \tag{23}$$

$$B = \frac{\dfrac{\rho^{(1)}}{\rho^{(2)}}\dfrac{C_p^{(1)}}{C_p^{(2)}}}{2\dfrac{\mu^{(1)}}{\mu^{(2)}}}\left[M^{(2)}\alpha^{(1)} + 2\frac{\mu^{(1)}}{\mu^{(2)}}v_m^{(2)*}\right]\alpha^{(1)} - M^{(2)}\alpha^{(1)}\left[1 - \frac{1}{2}\alpha^{(1)}\right] - [\alpha^{(1)}]^2[\ln\alpha^{(1)} - 1], \tag{24}$$

$$K = \frac{\rho^{(1)}C_p^{(1)}[T_0^{(1)}Q^{(1)} - I_1] + \rho^{(2)}C_p^{(2)}[T_0^{(2)}Q^{(2)} + K_LQ^{(2)} - I_2]}{\rho^{(1)}C_p^{(1)}Q^{(1)} + \rho^{(2)}C_p^{(2)}Q^{(2)}}, \tag{25}$$

$$L = K - K_L \tag{26}$$

where I_1, I_2 and K_L are as follows:

$$I_1 = \frac{\pi aN^2R^8}{128\mu^{(1)2}\alpha_t^{(1)}}[\alpha^{(1)}]^2\left\{\frac{7}{24}[M^{(1)}]^2[\alpha^{(1)}]^2 + \frac{7}{6}\frac{\mu^{(1)}}{\mu^{(2)}}M^{(1)}\alpha^{(1)}v_m^{(2)*} + \left[\frac{\mu^{(1)}}{\mu^{(2)}}v_m^{(2)*}\right]^2\right\}, \tag{27}$$

$$\begin{aligned} I_2 = \frac{\pi aN^2R^8}{128\mu^{(2)2}\alpha_t^{(2)}}\Bigg(\Bigg([M^{(2)}]^2\Bigg[\Bigg[\frac{7}{24} - [\alpha^{(1)}]^2\left\{1 - \frac{5}{6}\alpha^{(1)} + \frac{1}{8}[\alpha^{(1)}]^2\right\}\Bigg]\Bigg] \\ - M^{(2)}\Bigg[\Bigg[\frac{3}{2}B - \left(2B - \frac{25}{18}\right)\alpha^{(1)} + \frac{1}{2}B[\alpha^{(1)}]^2 - 3[\alpha^{(1)}]^3 + \frac{29}{18}[\alpha^{(1)}]^4 \\ + 2\alpha^{(1)}\left\{B - \frac{1}{2}B\alpha^{(1)} - [\alpha^{(1)}]^2 - \frac{5}{12}[\alpha^{(1)}]^2\right\}\ln\alpha^{(1)}\Bigg]\Bigg] \\ + 4B\alpha^{(1)} - \left(\frac{3}{2} - 4B\right)[\alpha^{(1)}]^2 - \frac{3}{2}[\alpha^{(1)}]^4 + [\alpha^{(1)}]^2\{4B + 3[\alpha^{(1)}]^2\}\ln\alpha^{(1)} \\ - [\alpha^{(1)}]^2\{2B + [\alpha^{(1)}]^2\}\ln^2\alpha^{(1)}\Bigg)\Bigg), \end{aligned} \tag{28}$$

$$\begin{aligned} K_L = \frac{1}{P^{(2)}}\cdot\Bigg[\Bigg[M^{(2)}\left\{\alpha^{(1)} - \frac{1}{4}[\alpha^{(1)}]^2\right\} + [\alpha^{(1)}]^2[\ln\alpha^{(1)} - 2] + B\ln\alpha^{(1)}\Bigg]\Bigg] \\ - \frac{1}{P^{(1)}}\cdot\left\{\frac{3}{4}M^{(1)}[\alpha^{(1)}]^2 + \frac{\mu^{(1)}}{\mu^{(2)}}v_m^{(2)*}\right\}, \end{aligned} \tag{29}$$

$Q^{(i)}$ are the volumetric flow rates of the liquids.

Heat flux distributions $q_F^{(i)}$ are derived from the temperature distributions as follows:

$$q_F^{(i)} = -k^{(i)}\frac{\partial T_F^{(i)}}{\partial r}. \tag{30}$$

Bulk temperatures $T_{BF}^{(i)}$ are derived by using the velocity profiles $v^{(i)}$ and the temperature disttibutions $T_F^{(i)}$, as follows:

$$T_{BF}^{(1)} = \frac{\int_0^{R_m} 2\pi r v^{(1)} T_F^{(1)} \, dr}{Q^{(1)}} , \quad [31]$$

$$T_{BF}^{(2)} = \frac{\int_{R_m}^{R} 2\pi r v^{(2)} T_F^{(2)} \, dr}{Q^{(2)}} . \quad [32]$$

Nusselt numbers $Nu_{BF}^{(i)}$ are derived according to the following definitions:

$$Nu_{BF}^{(1)} = \frac{q_m D_m}{k^{(1)}[T_{mF} - T_{BF}^{(1)}]} , \quad [33]$$

$$Nu_{BF}^{(2)} = \frac{q_w D}{k^{(2)}[T_{wF} - T_{BF}^{(2)}]} , \quad [34]$$

where q_m, D_m and T_{mF} are the heat flux, the diameter and the temperature at the interface and T_{wF} is the temperature at the wall. Expressions for $q_F^{(i)}$, $T_{BF}^{(i)}$ and $Nu_{BF}^{(i)}$ are presented by Fink (1975).

2.3 *Superposition solution*

The temperature field is taken as a superposition of fully developed (T_F) and developing (T_D) fields (Siegel, 1958):

$$T = T_F + T_D . \quad [35]$$

Subtraction of the differential equations and boundary conditions for T_F from those of the total temperature field T, yields the governing equations and boundary conditions for the developing temperature field T_D. The differential equations [1] and the boundary conditions [11]–[13] remain unchanged but boundary condition [14] and inlet conditions [15]–[16] are replaced by:

$$\text{at} \quad r = R \qquad \frac{\partial T_D^{(2)}}{\partial r} = 0, \quad [36]$$

$$\text{at} \quad z = 0 \qquad T_D^{(1)} = T_0^{(1)} - T_{F0}^{(1)}, \quad [37]$$

$$T_D^{(2)} = T_0^{(2)} - T_{F0}^{(2)}. \quad [38]$$

$T_{F0}^{(i)}$ are the fully developed temperature distributions with $z = 0$.

The above system of differential equations is solved by the orthogonal collocation method, using Jacobi polynomials as trial functions (Finlayson 1972; Villadsen & Michelsen 1975).

New radial coordinates are defined for the inner and for the outer liquid, in order to normalize the radial range in each of the two regions:

$$x^{(1)} = \left(\frac{r^*}{r_m^*}\right)^2, \quad [39]$$

$$x^{(2)} = \frac{r^* - r_m^*}{1 - r_m^*}, \quad [40]$$

where:

$$r_m^* = \frac{R_m}{R} = [\alpha^{(1)}]^{1/2}. \quad [41]$$

The definition of $x^{(1)}$ serves also the purpose of including the cylindrical symmetry boundary condition.

The differential equations and the boundary and initial conditions in the new coordinate system $x^{(i)}$ are:

$$\frac{1}{F^{(1)}}\frac{\partial}{\partial x^{(1)}}\left[x^{(1)}\frac{\partial T_D^{(1)}}{\partial x^{(1)}}\right]=\frac{\partial T_D^{1}}{\partial \lambda^{(1)}} \qquad 0\le x^{(1)}\le 1,\ \lambda^{(1)}>0, \tag{42}$$

$$\frac{1}{F^{(2)}}\frac{1}{x^{(2)}+\gamma}\frac{\partial}{\partial x^{(2)}}\left\{[x^{(2)}+\gamma]\frac{\partial T_D^{(2)}}{\partial x^{(2)}}\right\}=\frac{\partial T_D^{(2)}}{\partial \lambda^{(2)}} \qquad 0\le x^{(2)}\le 1,\ \lambda^{(2)}>0. \tag{43}$$

Boundary conditions:

at $x^{(1)}=1$ and $x^{(2)}=0$

$$T_D^{(1)}=T_D^{(2)}, \tag{44}$$

$$2\frac{k^{(1)}}{k^{(2)}}\frac{\partial T_D^{(1)}}{\partial x^{(1)}}=\gamma\frac{\partial T_D^{(2)}}{\partial x^{(2)}} \tag{45}$$

at $x^{(2)}=1$

$$\frac{\partial T_D^{(2)}}{\partial x^{(2)}}=0. \tag{46}$$

Initial conditions:

at $\lambda^{(1)}, \lambda^{(2)}=0$

$$T_D^{(1)}=T_0^{(1)}-T_{F0}^{(1)}, \tag{47}$$

$$T_D^{(2)}=T_0^{(2)}-T_{F0}^{(2)}, \tag{48}$$

where:

$$F^{(1)}=\frac{\alpha^{(1)}v^{(1)}}{4N^{(1)}}, \tag{49}$$

$$F^{(2)}=\frac{(1-r_m^*)^2v^{(2)}}{N^{(2)}}, \tag{50}$$

$$\gamma=\frac{r_m^*}{1-r_m^*}, \tag{51}$$

$$\lambda^{(i)}=\frac{\alpha_t^{(i)}}{N^{(i)}R^2}z. \tag{52}$$

Discretization of the L.H.S. of [42] at N_1 collocation points $x_i^{(1)}$ which are zeros of Jacobi polynomials (Villadsen & Michelsen 1975), yields:

$$\left.\frac{\partial T_D^{(1)}}{\partial \lambda^{(1)}}\right|_{x^{(1)}=x_i^{(1)}}=\sum_{j=1}^{N_1+1}D_{ij}Y_j \qquad i=1,2,\ldots,N_1, \tag{53}$$

where:

$$D_{ij}=\frac{x_i^{(1)}a_{ij}+b_{ij}}{F_i^{(1)}}, \tag{54}$$

$$F_i^{(1)}=F^{(1)}|_{x^{(1)}=x_i^{(1)}}. \tag{55}$$

a_{ij} and b_{ij} are obtained from the derivatives of the trial polynomials (Villadsen & Michelsen 1975) as follows:

$$\left.\frac{\partial^2 T_D^{(1)}}{\partial x^{(1)2}}\right|_{x^{(1)}=x_i^{(1)}}=\sum_{j=1}^{N_1+1}a_{ij}Y_j \qquad i=1,2,\ldots,N_1 \tag{56}$$

$$\left.\frac{\partial T_D^{(1)}}{\partial x^{(1)}}\right|_{x^{(1)}=x_i^{(1)}}=\sum_{j=1}^{N_1+1}b_{ij}Y_j \qquad i=1,2,\ldots,N_1 \tag{57}$$

Y_j are the temperatures of the inner liquid at the N_1 collocation points and the interface temperature.

Similarly, discretization of the L.H.S. of [43] at N_2 collocation points $x_i^{(2)}$ yields:

$$\left.\frac{\partial T_D^{(2)}}{\partial \lambda^{(2)}}\right|_{x^{(2)}=x_i^{(2)}} = \sum_{j=1}^{N_2+2} H_{ij} Z_j; \qquad i = 2, 3, \ldots, N_2+1 \tag{58}$$

where:

$$H_{ij} = \frac{l_{ij} + \dfrac{1}{x^{(2)}+\gamma} f_{ij}}{F_i^{(2)}}, \tag{59}$$

$$F_i^{(2)} = F^{(2)}|_{x^{(2)}=x_i^{(2)}}, \tag{60}$$

l_{ij} and f_{ij} are obtained in a similar way as a_{ij} and b_{ij}:

$$\left.\frac{\partial^2 T_D^{(2)}}{\partial x^{(2)2}}\right|_{x^{(2)}=x_i^{(2)}} = \sum_{j=1}^{N_2+2} l_{ij} Z_j \qquad i = 2, 3, \ldots, N_2+1, \tag{61}$$

$$\left.\frac{\partial T_D^{(2)}}{\partial x^{(2)}}\right|_{x^{(2)}=x_i^{(2)}} = \sum_{j=1}^{N_2+2} f_{ij} Z_j \qquad i = 2, 3, \ldots, N_2+1. \tag{62}$$

Z_j are the interface temperature, the temperatures at N_2 collocation points for the outer liquid and the wall temperature.

The boundary temperatures Y_{N_1+1}, Z_1 and Z_{N_2+2} are eliminated from [53] and [58] by using the three boundary conditions [44]–[46]. Details of the derivations are presented by Leib (1975) and the final system of equations is expressed as:

$$\frac{\partial \mathbf{T_D}}{\partial \lambda} = \boldsymbol{A}\mathbf{T_D} \tag{63}$$

$\boldsymbol{A}$ is a square matrix with dimensions $(N_1+N_2)\times(N_1+N_2)$, $\mathbf{T_D}$ is the vector of the temperatures at the N_1+N_2 collocation points and $\partial \mathbf{T_D}/\partial\lambda$ is the vector of the axial temperature gradients at the N_1+N_2 collocation points.

Equation [63] is a system of N_1+N_2 coupled first order differential equations uncoupled by diagonalization of the square matrix $\boldsymbol{A}$:

$$\boldsymbol{A} = \boldsymbol{Q}\boldsymbol{\Lambda}\boldsymbol{Q}^{-1} \tag{64}$$

$\boldsymbol{Q}$ is the matrix of the Eigenvectors of $\boldsymbol{A}$, $\boldsymbol{Q}^{-1}$ is the inverse of $\boldsymbol{Q}$ and $\boldsymbol{\Lambda}$ is the diagonal matrix of the Eigenvalues of $\boldsymbol{A}$. After some algebraic manipulations, [63] becomes:

$$\frac{\partial(\boldsymbol{Q}^{-1}\mathbf{T_D})}{\partial\lambda} = \boldsymbol{\Lambda}(\boldsymbol{Q}^{-1}\mathbf{T_D}). \tag{65}$$

Equation [65] is a system of N_1+N_2 uncoupled first order differential equations, directly solvable for $\mathbf{T_D}$, yielding:

$$\mathbf{T_D} = \boldsymbol{Q}\exp(\boldsymbol{\Lambda}\lambda)\boldsymbol{Q}^{-1}\mathbf{T_{D0}} \tag{66}$$

where use was made of the initial conditions [47]–[48], which in vectorial form are:

$$\text{at } \lambda = 0 \qquad \mathbf{T_D} = \mathbf{T_{D0}}. \tag{67}$$

It may be shown that [66] is equivalent to the classical Graetz solution for a developing temperature field in a tube with Eigenfunctions approximated by discrete eigenvectors of the matrix A.

Equation [66] gives the temperature distribution at $N_1 + N_2$ collocation points, together with the fully developed temperature T_F. At any other radial point, the temperature is determined by using the Lagrangian interpolation (Villadsen & Michelsen 1975).

The heat-flux distribution, according to the principle of superposition, is:

$$q^{(i)} = q_F^{(i)} + q_D^{(i)} \qquad [68]$$

where $q_D^{(i)}$ is derived by using [57] and [62] ($q_D^{(i)}$ is defined, as $q_F^{(i)}$, by [26]).

Bulk temperatures $T_{BD}^{(i)}$ are defined by [27] and [28]. $T_D^{(i)}$ being given at discrete collocation points, the integrals in these equations are best performed by a Radau quadrature (Villadsen & Michelsen 1975). The total bulk temperature follows from the principle of superposition:

$$T_B^{(i)} = T_{BF}^{(i)} + T_{BD}^{(i)}. \qquad [69]$$

Nusselt numbers are defined by [29] and [30], where total temperatures take the place of the fully developed temperatures.

Final expressions of total heat-flux distributions, bulk temperatures and Nusselt numbers are presented by Leib (1975).

The convergence of the superposition solution was tested for various Jacobi polynomials and for growing numbers of collocation points N_1 and N_2. The quickest convergence even at very short entry lengths, i.e. 0.1 diameters, was found with average values (bulk temperatures). Local values were found to converge beyond 10 diameters from the inlet, with N_1 and N_2 being each 16.

The superposition solution and the solution of the fully developed temperature field, although presented for uniform inlet temperatures, are suitable for arbitrary inlet temperature distributions $T_0(r)$.

2.4 *Entrance solution*

The approach used by Bird *et al.* (1960) for single-phase flow may be extended to the present two-phase flow system, by introducing the two-phase flow field.

Following Bird *et al.* (1960), the thermal boundary layer is assumed thin relative to the thickness of the outer liquid, so that the curvature of the tube may be ignored. It is possible then to change the cylindrical coordinate system to cartesian coordinates, thus simplifying the differential equations [1]. The velocity profile is reduced to a linear one, with the shape of the fully developed two-phase velocity profile at the wall of the tube. The above assumptions restrict the solution to very short entry lengths, where heat penetration is confined to the outer liquid alone. Thus, we need consider only the outer liquid.

The governing equations and boundary and initial conditions are:

$$\frac{\partial}{\partial \eta}\left[\frac{1}{\eta}\left(\frac{\partial \psi}{\partial \eta}\right)\right] = \frac{\partial \psi}{\partial \lambda}. \qquad [70]$$

Boundary conditions:

$$\text{at } \eta = 0 \qquad \psi = 1, \qquad [71]$$

$$\text{at } \eta = \infty \qquad \psi = 0. \qquad [72]$$

Initial condition:

$$\text{at } \lambda = 0 \qquad \psi = 0 \qquad [73]$$

where:

$$\psi = \frac{q}{q_w}, \tag{74}$$

$$\lambda = \frac{\alpha_t^{(2)}}{u_0 R^2} z, \tag{75}$$

$$\eta = \frac{y}{R}. \tag{76}$$

The slope of the linear profile u_0/R is calculated from the actual two-phase velocity profile, given by [3], according to:

$$u_0 = -R \left. \frac{dv^{(2)}}{dr} \right|_{r=R}. \tag{77}$$

Equation [70] is converted to an ordinary differential equation by the similarity variable X:

$$X = \frac{\eta}{\sqrt[3]{9\lambda}}. \tag{78}$$

Solution of the ordinary differential equation, gives the following expression for the temperature profile:

$$T^{(2)} = T_0^{(2)} + \frac{q_w R}{k^{(2)}} (9\lambda)^{1/3} \left\{ \frac{\exp(-X^3)}{\Gamma(2/3)} - X\left[1 - \frac{\Gamma[(2/3), X^3]}{\Gamma(2/3)}\right]\right\}. \tag{79}$$

$\Gamma(2/3)$ is the Gamma function and $\Gamma[(2/3), X^3]$ is the incomplete Gamma function, expressed as:

$$\Gamma[(2/3), X^3] = \int_0^X X \exp(-X^3)\, dX. \tag{80}$$

Details of the derivations are presented by Bird *et al.* (1960). However, in the present study, the two phase flow field is included through [77].

The thickness of the thermal boundary layer δ may be defined as

$$\frac{T^{(2)}|_{y=\delta} - T_0^{(2)}}{T^{(2)}\Big|_{y=0} - T_0^{(2)}} = 0.01. \tag{81}$$

Equation [81] is solved by a trial and error method (Leib, 1975) using tabulated values of $\Gamma[(2/3, X^3]$ (Abramowitz & Segun 1968), yielding:

$$\delta = 1.2228 \left[\frac{9R\alpha_t^{(2)}}{u_0}\right]^{1/3} z^{1/3}. \tag{82}$$

Bulk temperatures are determined according to:

$$T_B^{(2)} = \frac{\int_{R_m}^{R_\delta} 2\pi r v^{(2)} T_0^{(2)}\, dr + \int_{R_\delta}^{R} 2\pi r u^{(2)} T^{(2)}\, dr}{Q^{(2)}}, \tag{83}$$

where:

$$u^{(2)} = u_0 \frac{y}{R}, \tag{84}$$

$$R_\delta = R - \delta. \quad [85]$$

Nusselt numbers are determined according to [30].

Expressions for bulk temperatures and Nusselt numbers are presented by Leib (1975).

3. CALCULATED RESULTS

Results were calculated according to three respective models (entrance, fully developed and developing temperature fields), over the range of variables which were experimentally explored.

As described below, the system investigated was heat transfer to water and kerosene in annular flow, with the less heat conducting liquid flowing around the wall. Solutions were obtained for a heat flux of about 15,000 kcal/(hr m^2), a pipe diameter of 1.0 cm and a pipe length of about 1.0 m.

Table 1 summarizes input parameters and flow characteristics predicted by the undisturbed flow solution (Hasson *et al.* 1974). Reynolds numbers are defined according to Hasson *et al.* (1974) as follows:

$$Re^{(1)} = \frac{\rho^{(1)}|(v_{av}^{(1)} - v_m)|D_m}{\mu^{(1)}}, \quad [86]$$

$$Re^{(2)} = \frac{\rho^{(2)}v_{av}^{(2)}(D - D_m)}{\mu^{(2)}}. \quad [87]$$

$v_{av}^{(i)}$ are the average velocities of the liquids and v_m is the interfacial velocity. It has been found (Hasson *et al.* 1974, and further data to be published) that measured pressure drops and hold-ups are in agreement with the laminar flow analysis up to Reynolds numbers around 1700–2000 after which deviations from predictions progressively increase first moderately and then markedly.

Table 2 compares heat-transfer results at two dimensionless axial distances z^*, defined by:

$$z^* = \frac{z}{D}. \quad [88]$$

The dimensionless temperature difference is defined by:

$$\Delta T_C^{(i)*} = \frac{T^{(i)} - T_C}{T_w - T_C} \quad [89]$$

where T_C is the center line temperature.

Figures 2–4 depict the temperature profiles, the bulk temperatures and the outer liquid Nusselt numbers for conditions of run A2. Comparison of the superposition solution with the

Table 1. Input parameters and predicted flow characteristics

Run No.	$Q^{(1)}$ (litres/min)	$Q^{(2)}$ (litres/min)	$T_0^{(1)}$ (°C)	$T_0^{(2)}$ (°C)	$Re^{(1)}$	$Re^{(2)}$	$\alpha^{(1)}$	$-dp/dz$ (N/m^3)	$v_{av}^{(1)}$ (m/sec)	$v_{av}^{(2)}$ (m/sec)
A2	2.03	2.45	28.4	28.4	4431	2526	0.48	9508	0.897	1.000
B2	2.03	2.05	28.4	28.4	4294	2174	0.523	9552	0.823	0.913
C2	2.03	1.5	28.4	28.4	3675	1618	0.586	9617	0.735	0.769
A3	2.7	2.45	27.7	27.7	3166	2472	0.497	9592	1.154	1.033
B3	2.7	2.05	27.8	27.8	2851	2107	0.536	9628	1.068	0.938
C3	2.7	1.5	27.9	27.9	2326	1636	0.602	9678	0.952	0.8
A4	3.45	2.45	27.8	27.8	1833	2441	0.514	9676	1.423	1.071
B4	3.45	2.05	27.8	27.8	1491	2093	0.553	9704	1.324	0.973
C4	3.45	1.5	27.9	27.9	873	1644	0.617	9741	1.186	0.831
B5	2.7	2.05	28.5	51.9	4818	2637	0.572	9581	1.002	1.016

Table 2. Calculated heat transfer results at two entry lengths according to the various solutions

Run No.	$z^* = 75$				$z^* = 5000$							
	$Nu_B^{(2)}$		$\Delta T_{BC}^{(2)*}$		$Nu_B^{(2)}$		$Nu_B^{(1)}$		$\Delta T_{BC}^{(2)*}$		$\Delta T_{BC}^{(1)*}$	
	Entr.	Superp.	Entr.	Superp.	Superp.	Develop.	Superp.	Develop.	Superp.	Develop.	Superp.	Develop.
A2	22.67	21.09	0.0968	0.0962	10.66	10.64	11.9	11.85	0.4967	0.4982	0.0821	0.083
B2	23.22	21.56	0.1154	0.1147	11.76	11.76	11.87	11.85	0.508	0.5109	0.0935	0.094
C2	24.19	22.33	0.1552	0.1553	13.75	13.75	11.34	11.33	0.5324	0.5337	0.1161	0.1169
A3	22.96	21.41	0.0983	0.0992	10.85	10.82	10.03	9.91	0.518	0.5214	0.0988	0.1017
B3	23.44	21.79	0.1167	0.1167	11.9	11.89	9.86	9.77	0.5315	0.5357	0.1119	0.1142
C3	24.72	22.87	0.158	0.1589	14.14	14.14	9.53	9.46	0.5574	0.5584	0.1361	1.1378
A4	23.38	21.82	0.1001	0.1022	11.15	11.1	9.04	8.82	0.5319	0.5385	0.1087	0.1151
B4	23.86	22.22	0.1187	0.1187	12.24	12.22	8.87	8.68	0.5465	0.5518	0.1223	0.1281
C4	25.29	23.44	0.1608	0.1624	14.61	14.59	8.59	8.4	0.5724	0.5794	0.1455	0.1519
B5	25.48	21.79	0.3819	0.3107	13.23	13.21	10.99	10.9	0.5264	0.5268	0.1103	0.1124

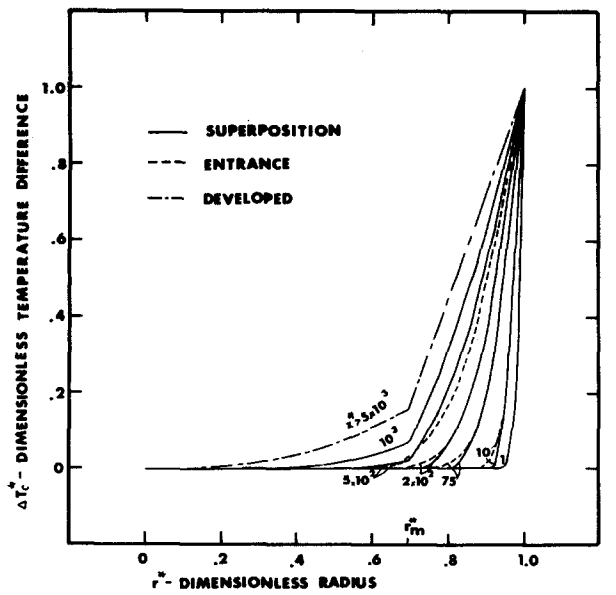

Figure 2. Comparison of temperature profiles according to the various solutions, with axial distance as parameter.

solution of the fully developed temperature field shows that the temperature becomes fully developed at an inlet length greater than 5000 diameters. This relatively large entry length is at least one order of magnitude greater than that encountered in single-phase flow, and is an interesting two-phase flow effect. It may be also noted from figures 2–4 that the entrance solution holds up to an inlet length of 100 diameters.

The comparison of Nusselt numbers and bulk temperatures given in Table 2 for inlet lengths of 75 diameters and 5000 diameters respectively, demonstrates the validity of the above results for all calculated conditions.

All runs given in tables 1 and 2 except the last one (B5) assume equal inlet fluid temperatures. A case of special interest is the system whereby the outer liquid is preheated. (One might wish to recycle the exit heated outer liquid to the pipe inlet of heat economy and better heat transfer to the inner liquid). The effects involved are demonstrated in figure 5. It is seen that above a certain inlet temperature difference, the outer phase may initially lose more heat to the inner liquid than it receives from the wall, thus going through a minimum temperature, before eventually heating-up again. This effect is also reflected in the temperature profile of figure 8, by the existence of an inflexion point in the outer phase region. The inflexion

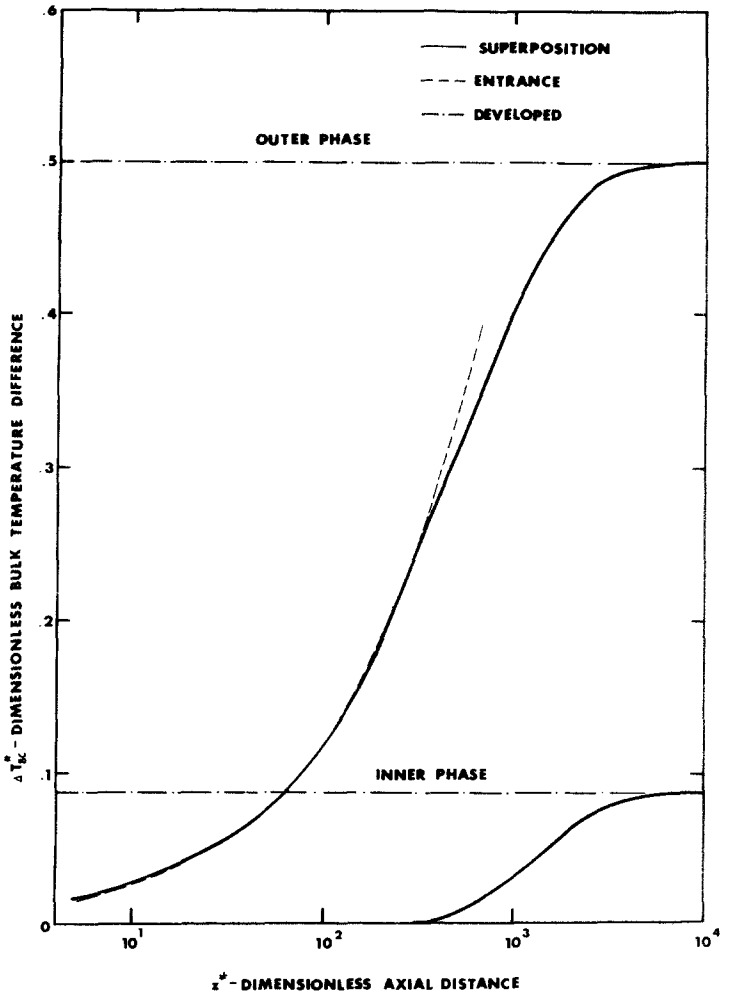

Figure 3. Comparison of bulk temperature differences according to the various solutions.

point results from the development of two thermal boundary layers in the outer phase—one adjacent to the wall and other adjacent to the interface. The inflexion point disappears at sufficiently large axial distances when the two thermal boundary layers reach each other.

Experimental evidence for this type of behaviour is presented later (figure 8).

4. EXPERIMENTAL OBSERVATIONS

The analytical study was complemented by experimental work carried out in the flow system described by Hasson *et al.* (1974) and adapted for heat transfer measurements by Leib (1975).

Measurements were taken with a well insulated brass tube, electrically heated by a heating tape around the wall, giving a heat flux of 15,000 kcal/(hr m^2). The pipe was provided with an inlet nozzle for achieving annular flow. Existence of annular flow was confirmed by visual observations at the short glass pipe sections at inlet and outlet. The pipe was of 1.0 cm I.D. and of 1.0 m length. Radial temperature profiles were measured with micro-miniature copper–constantan thermocouples, adjusted by a micrometric device with a precision of ± 0.1 mm. It was possible to obtain reliable temperature profiles at two cross-sections along the pipe, one at an entry length of 25 cm and the other at an entry length of 75 cm.

Table 1 gives the range of variables experimentally investigated. The flow rates studied correspond to a moderately disturbed annular flow pattern and very low drop entrainment (so-called region I, Hasson *et al.* 1974).

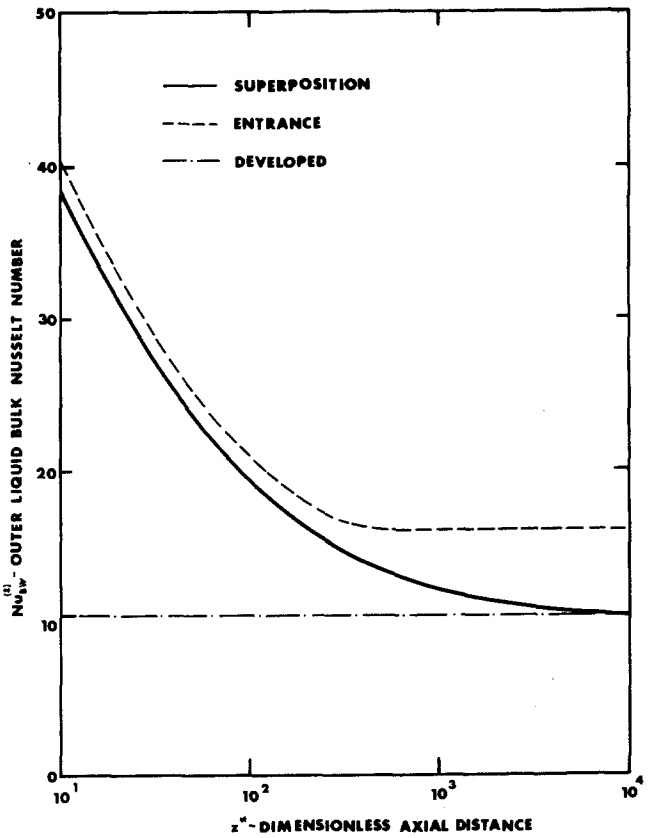

Figure 4. Comparison of outer liquid Nusselt numbers according to the various solutions.

The reliability of the experimental system was checked by single-phase flow heat-transfer measurements, with either water or kerosene flowing alone in the pipe. In all cases, single phase flow resulted in Reynolds numbers in the turbulent region (4200–11,000). As shown in figure 6, there was good agreement between measured values and values predicted from the well-established heat transfer correlations:

$$Nu_B = 0.034 Re^{0.8} Pr^{1/3} \left(\frac{\mu_w}{\mu}\right)^{-0.14} \left(\frac{z}{D}\right)^{-0.054} \quad \text{(for } z = 0.25 \text{ m)}, \qquad [90]$$

$$Nu_B = 0.023 Re^{0.8} Pr^{1/3} \left(\frac{\mu_w}{\mu}\right)^{-0.14} \quad \text{(for } z = 0.75 \text{ m)} \qquad [91]$$

where Re is the conventional single phase Reynolds number and μ_w is the viscosity at the wall temperature.

Figure 7 compares observed temperature profiles with profiles predicted by the superposition solution. It also gives the measured temperature profiles for the flow of water alone at the same water flow rate used for the two-phase flow run, other conditions remaining the same. These results typify the conclusions reached from the heat-transfer measurements.

It is observed that for two-phase flow, the experimental temperature profiles are markedly flatter than predicted by the undisturbed heat-transfer model. From a practical point of view, when the objective is to heat the inner liquid (water), the effect of the kerosene is to act as a thermal insulating layer. As seen from figure 7, while the presence of kerosene adversely affects the water temperature profile, it does so to a lesser extent than predicted by the undisturbed heat-transfer analysis. Thus the waviness counteracts to a certain extent the insulating effect.

Theoretical analysis predicts that one might entirely overcome the thermal insulating effect

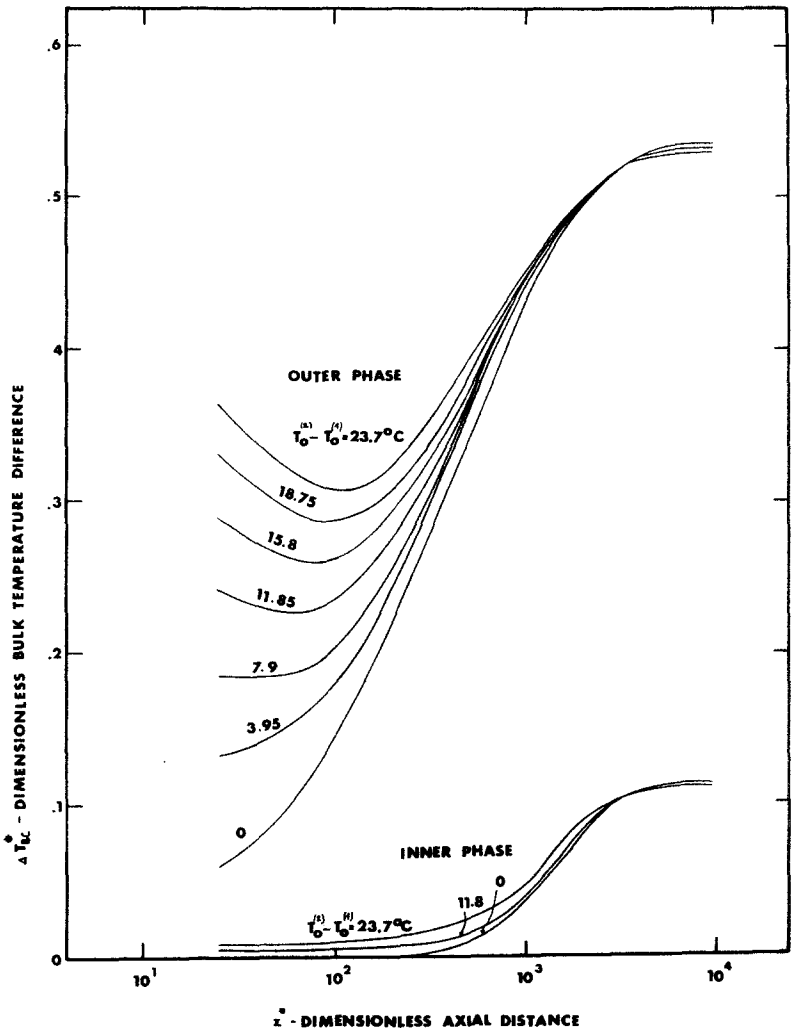

Figure 5. Effect of the inlet temperature difference on bulk temperatures of the two phases along the pipe.

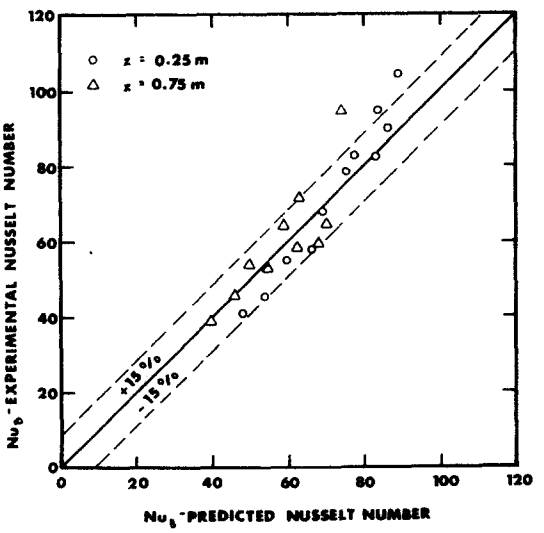

Figure 6. Comparison of observed and predicted Nusselt numbers for single phase flow of water and kerosene.

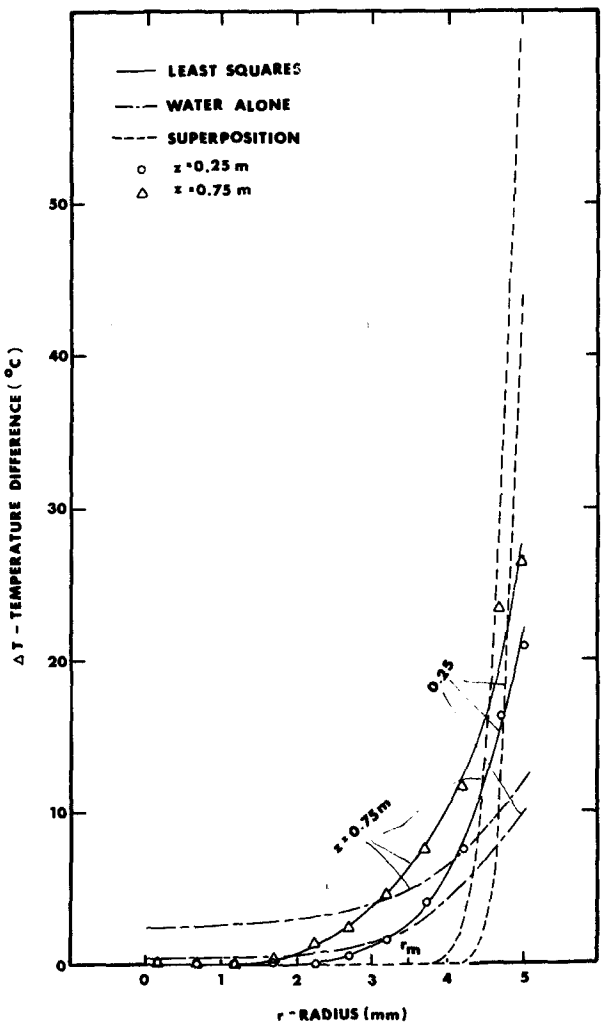

Figure 7. Comparison of observed and predicted temperature profiles (Run A2).

of the kerosene, by recycling the hot exit kerosene to the inlet of the pipe. An overall energy balance may be written as follows:

$$\rho^{(1)}C_p^{(1)}Q^{(1)}\Delta T_B^{(1)} = \rho^{(1)}C_p^{(1)}Q^{(1)}\Delta T_B^{(1)\prime} + \rho^{(2)}C_p^{(2)}Q^{(2)}\Delta T_B^{(2)}. \qquad [92]$$

$\Delta T_B^{(i)}$ is the bulk temperature difference between inlet and an axial distance z. The L.H.S. of [92] is the heat balance for single-phase flow of water, whereas the R.H.S. is the heat balance for annular water–kerosene flow, at the same flow rate of water and at the same heat flux at the wall. If $\Delta T_B^{(2)} = 0$, then $\Delta T_B^{(1)} = \Delta T_B^{(1)\prime}$, or, the same amount of heat may be transferred to water in the water–kerosene system as in single-phase flow of water, with the same pipe length. Referring to figure 5, it is seen that for curves with minima in the bulk temperature difference of the outer phase, $\Delta T_B^{(2)}$ may be made zero by choosing the appropriate outlet axial position.

Indirect experimental support to this effect is demonstrated in figure 8. As mentioned before, the analysis predicts that under preheated outer liquid conditions (i.e. unequal inlet temperatures), the temperature profile has an inflexion point in the outer phase region. Figure 8 shows that despite the flattening effect of the waves, the existence of an inflexion point is experimentally observed.

Because of experimental and theoretical difficulties, it was not possible to extract measurements of inner liquid Nusselt numbers. Outer liquid Nusselt numbers are easier to

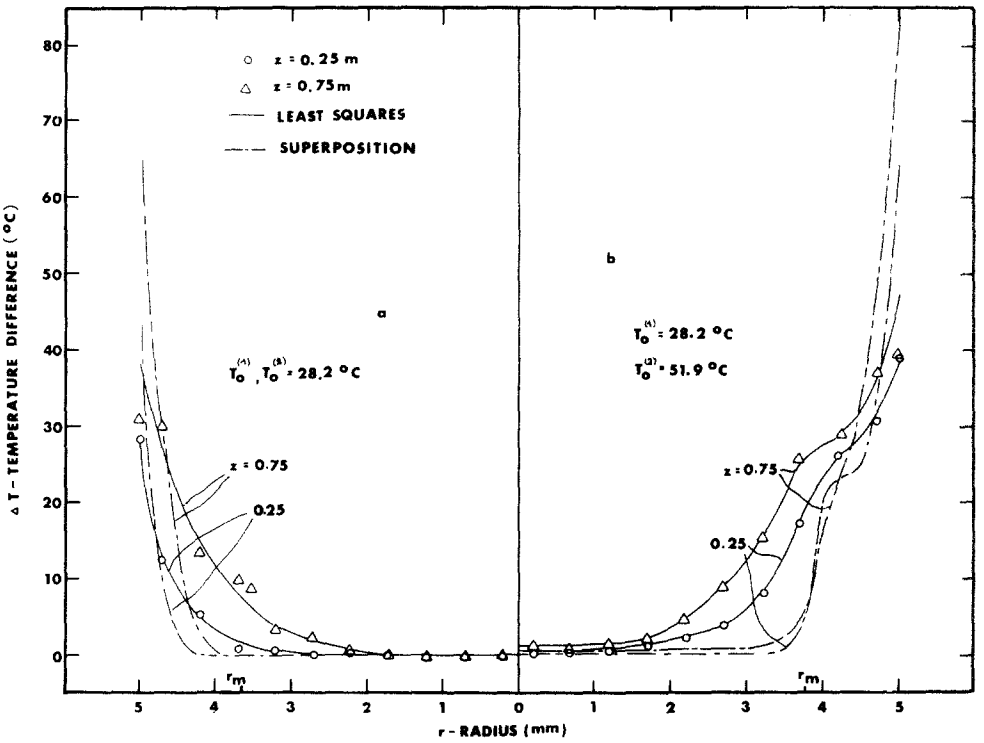

Figure 8. Comparison of observed and predicted temperature profiles: (a) Kerosene and water at same inlet temperature (Run B3). (b) Kerosene at a higher inlet temperature than water (Run B5).

obtain and values extracted from the temperature profiles are given in table 3. It is seen that they are 40–320% higher than predicted by the undisturbed laminar heat-transfer analysis, with a clear trend for increasing deviations as the outer liquid Reynolds number increases. The data of table 2 can be reasonably correlated by the empirical equation:

$$\frac{Nu^{(2)}_{exp}}{Nu^{(2)}_{theo}} = 1.5527 \times 10^{-4} Re^{(2)} \cdot z^{*0.3738} + 1. \qquad [93]$$

Table 3. Comparison of observed and predicted outer liquid Nusselt numbers

z (m)	Exp. No.	$Re^{(2)}$	$Nu_B^{(2)}$ Exptl.	$Nu_B^{(2)}$ Predicted	Deviation % Exptl. from Predicted
0.25	A2	2526	85.08	29.43	189
	B2	2174	68.49	29.82	130
	C2	1618	51.87	30.2	72
	A3	2472	74.15	29.79	149
	B3	2107	54.88	30.01	83
	C3	1636	42.91	30.77	39
	A4	2441	95.42	30.25	215
	B4	2093	69.49	30.53	128
	C4	1644	46.26	31.43	47
	B5	2637	93.91	30.49	208
0.75	A2	2526	77.26	21.09	266
	B2	2174	53.38	21.56	147
	C2	1618	51.28	22.33	130
	A3	2472	59.58	21.41	178
	B3	2107	52.78	21.79	142
	C3	1636	43.4	22.87	90
	A4	2441	92.09	21.82	322
	B4	2093	69.78	22.22	214
	C4	1644	39.91	23.44	70
	B5	2637	76.39	21.79	250

In fact, it would seem from this result and further study of the flow transition criterion which is in progress, that the experimental data of this work fall in the early region of transition from laminarity.

5. CONCLUSIONS

Solutions for heat transfer in annular laminar undisturbed two-phase flow with constant heat flux conditions have been derived. It is shown, that a superposition model adequately describes the temperature field over the whole length of the heated pipe. The fully developed temperature field solution is found to be applicable at much larger entry lengths than encountered in single phase flow.

Heat transfer measurements show that for low viscosity liquids, such as water and kerosene, the interfacial waviness leads to significant deviations from the predicted undisturbed heat transfer. From a practical point of view, the interfacial waviness acts to augment the heat transfer, counteracting the insulating effect of kerosene when it is desired to heat the inner liquid, water. Measurements of the Nusselt number for the outer phase were between 40–320% higher than predicted by the analysis.

Acknowledgement—This work forms part of theses submitted to the Senate of the Technion–Israel Institute of Technology, one by T. M. Leib in partial fulfillment of the requirements for the M.Sc. degree and the other by M. Fink in partial fulfillment of the requirements for the Ph.D. degree. The authors are indebted to Prof. J. Villadsen for stimulating discussions.

REFERENCES

ABRAMOWITZ, M. & STEGUN, I. A. 1968 *Handbook of Mathematical Functions.* Dover Publications, New York.

BENTWICH, M. & SIDEMAN, S. 1964 Temperature distribution and heat transfer in annular two-phase (liquid–liquid) flow. *Can. J. Chem. Engng* **42**, 9–13.

BIRD, R. B., STEWART, W. E. & LIGHTFOOT, E. N. 1960 *Transport Phenomena.* Wiley, New York.

FINK, M. 1975 Flow and heat transfer of two immiscible liquids. Ph.D. Thesis, Technion-IIT, Department of Chemical Engineering.

FINLAYSON, B. A. 1972 *The Method of Weighted Residuals and Variational Principles.* Academic Press, New York.

HASSON, D., ORELL, A. & FINK, M. 1974 A study of vertical annular liquid–liquid flow—Part I, laminar conditions. Paper No. A5, Multi-Phase Flow Systems Symp., Inst. Chem. Engng, Symp. Ser. No. 38, Glasgow, 1–15.

LEIB, T. M. 1975 Heat transfer in annular flow of two immiscible liquids. M.Sc. Thesis, Technion-IIT, Department of Chemical Engineering.

SIDEMAN, S. & PECK, R. E. 1966 Graphical solution for heat transfer in two-phase laminar flow. *Israel J. Tech.* **5**, 203–210.

SIEGEL, R., SPARROW, E. M., HALLMAN, T. M. 1958 Steady laminar heat transfer in a circular tube with prescribed wall heat flux. *Appl. Sci. Res.* **A7**, 386–392.

VILLADSEN, J. & MICHELSEN, M. L. 1975 Solution of differential equation models by polynomial approximations. Instituttet for Kemiteknik, Danmarks Tekniske Hojskole.